JOURNAL OF THEORETICAL
AND APPLIED MECHANICS
https://doi.org/10.15632/jtam-pl/213898
ONLINE FIRST

VIBRATION FATIGUE BEHAVIOUR ANALYSIS OF THE CRACKED PLATE UNDER A UNIFORM TEMPERATURE FIELD

Yijiang MA*, Zijie ZOU, Jinfeng CHEN, Renjie SHEN

School of Naval Architecture and Ocean Engineering, Jiangsu University of Science and Technology, China
*corresponding author, *yima@nuaa.edu.cn*

For the thermal fatigue problem of the hypersonic aircraft's plate, a loose coupling analysis method is proposed to conduct vibration fatigue behaviour analysis of the cracked plate under a uniform temperature field. The temperature field is converted into additional loads, and the interaction mechanism between thermal coupling and crack propagation is explored. The modal, dynamic response and fatigue life analyses are conducted synchronously. The numerical simulation method is applied to verify this theoretical method. The results indicate that the analytical method proposed has sufficient computational accuracy, and the influence of the temperature field on vibration fatigue behaviour cannot be ignored.

Keywords: crack; temperature field; vibration fatigue behaviour; loose coupling analysis method.

1. Introduction

Hypersonic aircraft refers to the aircraft that travel at speeds exceeding 5 Mach. These types of aircraft have revolutionary potential in military, aerospace, and civilian fields due to extremely high speed, but also face technological problems. During prolonged hypersonic flights, aircraft fuselage plates generate extremely high temperatures due to air friction, posing significant challenges to the dynamic design and thermal protection. In a high-temperature and high-frequency vibration environment, there is an interaction between thermal coupling and crack propagation. Therefore, conducting the vibration fatigue behaviour analysis of the plate under a uniform temperature field has high engineering value.

Vibration fatigue behaviour analysis includes three parts: modal analysis, dynamic response analysis, and fatigue life analysis. In modal analysis, scholars have conducted extensive research work. Based on Kirchhoff's thin plate theory, Huang *et al.* (2018) derived the displacement tolerance function of a thin plate with elastic boundary conditions, and conducted modal analysis of the cracked rectangular plate using the Rayleigh-Ritz method. Xue and Wang (2019) used the Kirchhoff plate theory to describe the singularity of the stress field at the crack tip through a special allowable function, and the Ritz method was applied to investigate the influence of cracks on modal behaviour. Moradi *et al.* (2019) derived the vibration differential equation of a cracked plate based on the Mindlin plate theory, and analysed the influence of load and crack on a model of the plate by the differential quadrature element method. Heo *et al.* (2020) validated the boundary dynamics Mindlin plate equation through numerical methods, and conducted the free vibration analysis of the cracked plate. Song *et al.* (2022) derived the allowable function within the Kirchhoff plate theory framework based on Jacobi orthogonal polynomials, and applied the Ritz method to analyse the free vibration of a cracked polygonal thin plate. Dynamic response analysis mainly investigates the vibration response of the plate under external excitation. Useche (2020) established a numerical model of cracks by the double boundary ele-

ment equation, and proposed a method to investigate the bending vibration response of cracked plates based on the double reciprocity boundary element method. Based on the Kirchhoff plate theory, Jalili and Daneshmehr (2018) established a non-linear model of cracked plates and investigated the time-domain response of cracked plates characterized. Motaharifar *et al.* (2020) applied an improved line spring model to simulate through cracks, and conducted non-linear vibration response analysis of cracked von Kármán plates. Based on the Mindlin plate theory, Xue *et al.* (2020) simulated the stress field at the crack tip by angle displacement tolerance functions, and studied the non-linear vibration response of the cracked plate using Hamilton's principle. In fatigue life analysis, scholars have proposed various analytical methods. Jameel and Harmain (2019) applied the meshless Galerkin method to discretize the crack area, and proposed a fatigue crack propagation and life prediction method for a cracked plate. Ilie and Ince (2022) established the numerical model of a cracked plate using the ANSYS reduced order model and embedded the Paris equation into the fatigue crack growth module to conduct vibration fatigue life analysis. Tazoe *et al.* (2020) simplified cracks into a set of particle voids and proposed a crack propagation algorithm based on smooth particle fluid mechanics to analyse the crack propagation behaviour. Yadzhak *et al.* (2022) established a deformation parameter model for

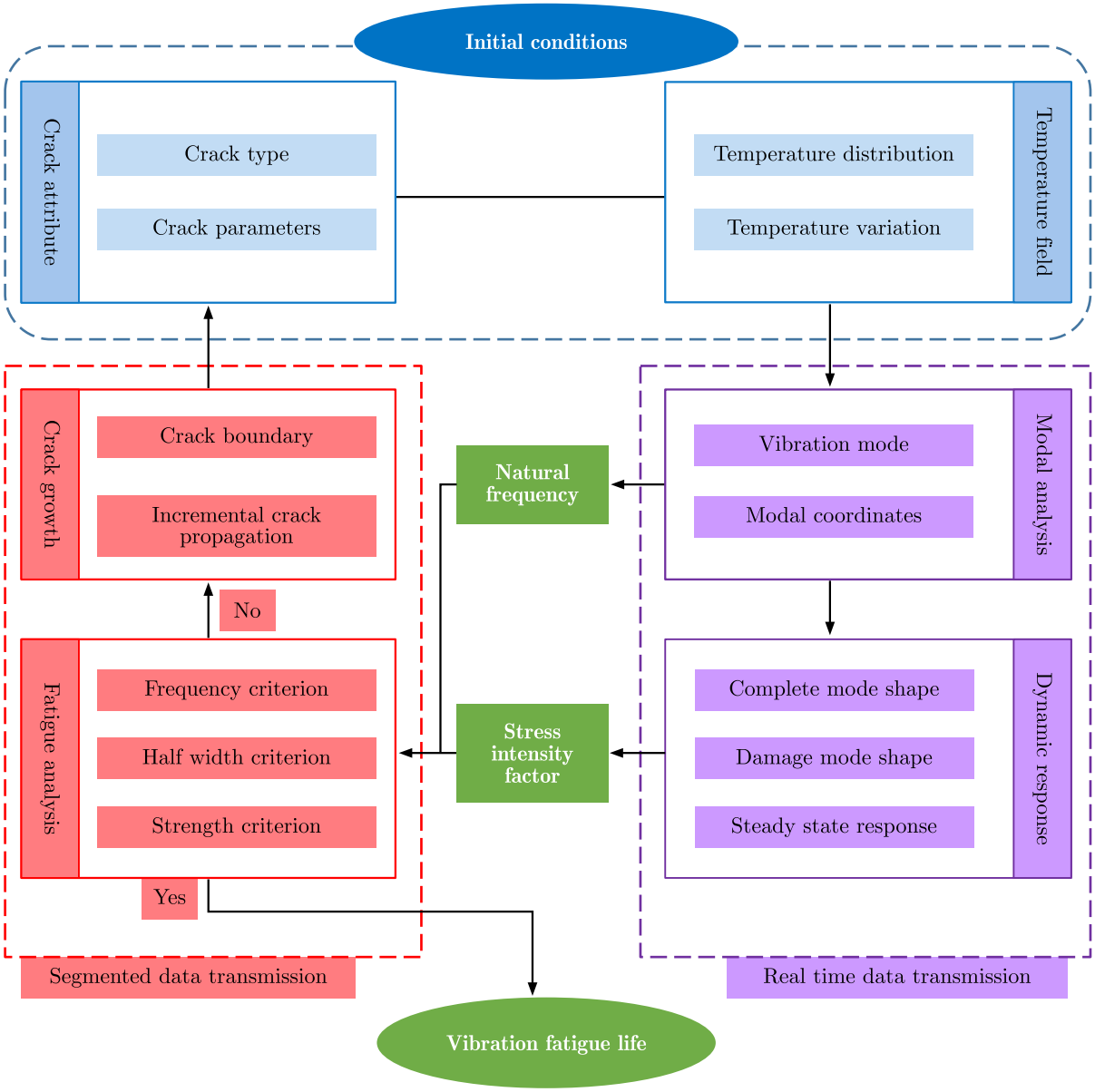

Fig. 1. Research process on vibration fatigue behaviour of the cracked plate.

crack tip opening displacement based on the energy method, and studied the crack propagation law under type II and III mixed loads to determine the fatigue life. The aforementioned research proposes multiple methods for vibration fatigue behaviour analysis of the cracked plate at room temperature, but does not consider the influence of temperature field distribution. The vibration fatigue behaviour analysis method in a normal temperature environment is not applicable to a variable temperature field environment.

In this paper, a loose coupling analysis method is proposed to investigate the vibration fatigue behaviour of the cracked plate. Based on the plate constitutive equation, the temperature field and stress field distribution can be investigated. Considering the interaction between thermal coupling and crack propagation, the additional thermal stress matrix and thermal deformation stiffness matrix can be derived. According to the Paris equation, the influence of the temperature field on the plate's fatigue life can be analysed. Based on the thermal stress and thermal modal analysis, the influence of temperature on vibration fatigue life is investigated, and the possibility of health monitoring of plates in service is provided. The research process of the loose coupling analysis method is shown in Fig. 1.

2. Vibration fatigue behaviour analysis

2.1. Vibration differential equation

Assumptions of the thin plate are as follows: the material is fully elastic, homogeneous, and isotropic; the thickness of the thin plate is uniform and much smaller than the other sizes; all strain components are small enough and satisfy Hooke's law; all transverse normal stress components and shear deformations, and the cross-sections satisfy the plane assumption; the moment of inertia and shearing forces of the plate are neglected. Based on the Kirchhoff plate theory (Israr, 2008), the vibration differential equation of the cracked plate can be expressed as follows:

$$\rho h\frac{\partial^2 w}{\partial t^2}+D_T\left(\frac{\partial^4 w}{\partial x^4}+2\frac{\partial^4 w}{\partial x^2\partial y^2}+\frac{\partial^4 w}{\partial y^4}\right)=n_x\frac{\partial^2 w}{\partial x^2}+2n_{xy}\frac{\partial^2 w}{\partial x\partial y}+n_y\frac{\partial^2 w}{\partial y^2}+\frac{\partial^2\overline{M_x}}{\partial x^2}+\frac{\partial^2\overline{M_y}}{\partial y^2}+\overline{n_x}\frac{\partial^2 w}{\partial x^2}+\overline{n_y}\frac{\partial^2 w}{\partial y^2}+P_z, \tag{2.1}$$

where $D_T=E_T h^3/12\left(1-v^2\right)$ is the flexural rigidity, w is the displacement in the z-direction of the mid-surface, ρ is the density, h is the thickness, E_T is the elastic modulus at different temperatures, v is Poisson's ratio and t is time, $\overline{n_x}$ and $\overline{n_y}$ are unit length additional surface forces in x- and y-axis directions caused by cracks, n_x and n_y are unit length additional surface forces in x- and y-axis directions caused by temperature changes, $\overline{M_x}$ and $\overline{M_y}$ are the unit length additional bending moments in the x- and y-axis directions caused by cracks, P_z is the external load on the plate.

Let us assume that $P_z=0$, and Eq. (2.1) becomes the free vibration differential equation. The crack is parallel to the x-axis and only the additional surface load n_x acts, affected by temperature. Therefore, Eq. (2.1) can be simplified:

$$\rho h\frac{\partial^2 w}{\partial t^2}+D_T\left(\frac{\partial^4 w}{\partial x^4}+2\frac{\partial^4 w}{\partial x^2\partial y^2}+\frac{\partial^4 w}{\partial y^4}\right)=n_x\frac{\partial^2 w}{\partial x^2}+\frac{\partial^2\overline{M_y}}{\partial y^2}+\overline{n_y}\frac{\partial^2 w}{\partial y^2}+P_z. \tag{2.2}$$

According to the singularity of the stress field at the crack tip, relationships between the nominal tensile stress and bending stress at the crack location and the nominal tensile stress and bending stress away from the crack location are as follows (Rice & Levy, 1972):

$$\sigma=[(1+\gamma\alpha_{bb})\sigma_\infty-\eta\alpha_{tb}\sigma_{b\infty}]/Q, \tag{2.3}$$

$$\sigma_{bb}=[-\gamma\alpha_{tb}\sigma_\infty+(1+\eta\alpha_{tt})\sigma_{b\infty}]/Q, \tag{2.4}$$

$$\begin{cases} \alpha_{tt} = 290.18\xi^{10} - 460.87\xi^{9} + 437.12\xi^{8} - 211.98\xi^{7} \\ \qquad + 99.19\xi^{6} - 33.64\xi^{5} + 18.6\xi^{4} - 0.54\xi^{3} + 1.97\xi^{2}, \\ \alpha_{bb} = 61.58\xi^{10} - 127.86\xi^{9} + 147.8\xi^{8} - 103.66\xi^{7} \\ \qquad + 63.77\xi^{6} - 31.34\xi^{5} + 14.46\xi^{4} - 3.29\xi^{3} + 1.98\xi^{2}, \\ \alpha_{tb} = 133.68\xi^{10} - 244.67\xi^{9} + 257.08\xi^{8} - 153.95\xi^{7} \\ \qquad + 84.07\xi^{6} - 34.87\xi^{5} + 16.0\xi^{4} - 1.91\xi^{3} + 1.97\xi^{2}, \end{cases} \tag{2.5}$$

where σ, σ_{bb} are the nominal tensile stress and bending stress at the crack location, σ_{∞}, $\sigma_{b\infty}$ are the nominal tensile stress and bending stress away from crack location, $\eta = \left(1-\nu^2\right)h/(2a)$, $\gamma = 3\,(3+\nu)\,(1-\nu)h/(2a)$, $Q = (1+\eta\alpha_{tt})\,(1+\gamma\alpha_{bb}) - \eta\gamma(\alpha_{tb})^2$, α_{bb}, α_{tt}, and α_{tb} are the local flexibility caused by cracks, a is the half width of the crack, ξ is the relative depth of the crack.

In fact, σ_{∞}, $\sigma_{b\infty}$, and the nominal stress magnitude are consistent with the absence of cracks at the crack location, and are expressed as follows:

$$\sigma_{\infty} = N_{\infty}/h = \int_{-h/2}^{h/2} (\tau_{ij}(x,0,z)/h)\,\mathrm{d}z, \tag{2.6}$$

$$\sigma_{b\infty} = 6M_{\infty}/h^2 = \int_{-h/2}^{h/2} (6z\tau_{ij}(x,0,z)/h^2)\,\mathrm{d}z, \tag{2.7}$$

where N_{∞} and M_{∞} are the tension and bending moment per unit length in the y-axis direction, respectively, when $y=0$, $\tau_{ij}(x,0,z)$ is the stress on the cross-section when $y=0$.

By replacing nominal tensile stress and nominal bending stress with tension and the bending moment, the additional tension and bending moment caused by cracks can be obtained as follows:

$$\overline{n_y} = [-(1+\gamma\alpha_{bb})N_{\infty} + 6\eta\alpha_{tb}M_{\infty}/h]/Q, \tag{2.8}$$

$$\overline{M_y} = [\gamma\alpha_{tb}hN_{\infty}/6 - (1+\eta\alpha_{tt})M_{\infty}]/Q. \tag{2.9}$$

Let us substitute Eqs. (2.8) and (2.9) into Eq. (2.2), and Eq. (2.2) can be simplified as follows:

$$\begin{aligned} D_T\left(\frac{\partial^4 w}{\partial x^4} + 2\frac{\partial^4 w}{\partial x^2\partial y^2} + \frac{\partial^4 w}{\partial y^4}\right) = & -\rho h\frac{\partial^2 w}{\partial t^2} + n_x\frac{\partial^2 w}{\partial x^2} - \phi N_{\infty}\frac{\partial^2 w}{\partial y^2} \\ & - \varphi\frac{\partial^2 M_{\infty}}{\partial y^2} + \lambda M_{\infty}\frac{\partial^2 w}{\partial y^2}, \end{aligned} \tag{2.10}$$

where N_{∞} is determined by the middle surface strain, M_{∞} is determined by internal force conditions of the Kirchhoff plate, other parameters are as follows: $M_{\infty} = -D_T(\partial^2 w/\partial y^2 + \nu\partial^2 w/\partial x^2)$, $\phi = (1+\gamma\alpha_{bb})/Q$, $\varphi = (1+\eta\alpha_{tt})/Q$, $\lambda = 6\eta\alpha_{tb}/(hQ)$.

2.2. Modal and dynamic response analysis

In order to simplify the analysis process, the influence of high-order modes is ignored, and the cracked plate is simplified into a single degree of freedom system by the Galerkin method. The general solution of the vibration differential equation for the cracked plate is as follows:

$$w(x,y,t) = \sum_{q=1}^{\infty}\sum_{p=1}^{\infty} A_{pq}X_pY_q\psi_{pq}(t), \tag{2.11}$$

where X_p and Y_q are vibration mode functions of the cracked plate, A_{pq} is the first-order amplitude, $\psi_{pq}(t)$ is the modal coordinate function of the cracked plate.

Convert the horizontally concentrated load into a uniformly distributed load by a δ function:

$$\overline{P_z} = P_0(t)\delta(x - x_0)\delta(y - y_0). \tag{2.12}$$

Let us substitute Eqs. (2.11) and (2.12) into Eq. (2.10), and Eq. (2.10) can be simplified as follows:

$$\begin{aligned}\frac{\rho h\ddot{\psi}_{pq}A_{pq}X_pY_q}{D_T} + [(Y_qX_p^{(4)} + 2X_p''Y_q'' + X_pY_q^{(4)}) - \varphi(X_pY_q^{(4)} + \nu X_p''Y_q'')]A_{pq}\psi_{pq} \\ + \lambda[X_p^2(Y_q'')^2 + \nu X_pY_qX_p''Y_q'']A_{pq}^2\psi_{pq}^2 + \frac{(-n_xX_p''Y_q + \phi N_\infty X_pY_q'')A_{pq}\psi_{pq}}{D_T} \\ = \frac{P_0(t)\delta(x - x_0)\delta(y - y_0)}{D_T}.\end{aligned} \tag{2.13}$$

Based on the strain energy caused by the second invariant of the applied surface strain, Berger (1955) determined the deformation of the same magnitude, and the surface load n_x and N_∞ can be obtained in the following way:

$$\begin{cases} n_x = D_TF_{1pq}A_{pq}^2\psi_{pq}^2, \\ N_\infty = D_TF_{2pq}A_{pq}^2\psi_{pq}^2, \end{cases} \tag{2.14}$$

$$\begin{cases} F_{1pq} = \dfrac{6}{h^2l_1l_2}\displaystyle\sum_{q=1}^{\infty}\sum_{p=1}^{\infty}\int_0^{l_1}\int_0^{l_2}\left[(X_p')^2Y_q^2 + \nu(Y_q')^2X_p^2\right]\mathrm{d}x\,\mathrm{d}y, \\ F_{2pq} = \dfrac{6}{h^2l_1l_2}\displaystyle\sum_{q=1}^{\infty}\sum_{p=1}^{\infty}\int_0^{l_1}\int_0^{l_2}\left[(Y_q')^2X_p^2 + \nu(X_p')^2Y_q^2\right]\mathrm{d}x\,\mathrm{d}y. \end{cases} \tag{2.15}$$

Let us substitute Eq. (2.14) into Eq. (2.13), and integrate Eq. (2.13) within the plate area:

$$M_{pq}\ddot{\psi}_{pq} + K_{pq}\psi_{pq} + H_{pq}\psi_{pq}^2 + G_{pq}\psi_{pq}^3 = P_{pq}, \tag{2.16}$$

$$\begin{cases} M_{pq} = \dfrac{\rho h}{D_T}\displaystyle\sum_{q=1}^{\infty}\sum_{p=1}^{\infty}A_{pq}\int_0^{l_1}\int_0^{l_2}X_p^2Y_q^2\,\mathrm{d}x\,\mathrm{d}y, \\ K_{pq} = \displaystyle\sum_{q=1}^{\infty}\sum_{p=1}^{\infty}A_{pq}\int_0^{l_1}\int_0^{l_2}\left[-\varphi(X_pY_q'''' + \nu X_p''Y_q'') + Y_qX_p'''' \right. \\ \qquad \left. + 2X_p''Y_q'' + X_pY_q''''\right]X_pY_q\,\mathrm{d}x\,\mathrm{d}y, \\ H_{pq} = \displaystyle\sum_{q=1}^{\infty}\sum_{p=1}^{\infty}\lambda A_{pq}^2\int_0^{l_1}\int_0^{l_2}X_pY_q\left[(X_pY_q'')^2 + \nu X_p''Y_qX_pY_q''\right]\mathrm{d}x\,\mathrm{d}y, \\ G_{pq} = \displaystyle\sum_{q=1}^{\infty}\sum_{p=1}^{\infty}A_{pq}^3\int_0^{l_1}\int_0^{l_2}X_pY_q\left(-F_{1pq}X_p''Y_q + \phi F_{2pq}X_pY_q''\right)\mathrm{d}x\,\mathrm{d}y, \\ P_{pq} = P_0(t)Q_{pq}/D_T, \\ Q_{pq} = X_p(x_0)Y_q(y_0), \end{cases} \tag{2.17}$$

where M_{pq} is the generalized mass, K_{pq} is the generalized stiffness, H_{pq} is the quadratic non-linear term, G_{pq} is the cubic non-linear term, P_{pq} is the generalized external load.

The vibration differential equation of the cracked plate under sinusoidal excitation $P_0(t) = p\cos(\Omega_{pq}t)$ is transformed into:

$$\ddot{\psi}_{pq} + \omega_{pq}^2\psi_{pq} + \alpha_{pq}\psi_{pq}^2 + \beta_{pq}\psi_{pq}^3 = \chi_{pq}p\cos(\Omega_{pq}t)/D_T, \tag{2.18}$$

where $\omega_{pq} = \sqrt{K_{pq}/M_{pq}}$ is the generalized natural frequency, $\alpha_{pq} = H_{pq}/M_{pq}$, $\beta_{pq} = G_{pq}/M_{pq}$, $\chi_{pq} = Q_{pq}/M_{pq}$.

2.3. Fatigue life analysis

Based on the coupling degree between thermal coupling and fatigue crack propagation, this paper makes the following assumptions: assuming that the time domain is discretized according to the external excitation period, the geometric sizes of the fatigue crack remain unchanged at each time step, and the fatigue crack pattern expands at the moment when each time step ends. Based on this assumption, the temperature field and stress field are in real-time data transmission form, while the analysis of fatigue crack propagation is in segmented data transmission form (data transmission occurs once at the end of each time step). Therefore, a loose coupling analysis method is proposed to carry out modal, dynamic response, and vibration fatigue life analysis of the cracked plate at each time step simultaneously, while achieving decoupling of stress and temperature fields in thin plate structures.

Under normal circumstances, the relationship between the dynamic stress intensity factor at the crack tip and the crack depth can be expressed as

$$\Delta K = F(\xi)\Delta\sigma_d\sqrt{\pi a}, \tag{2.19}$$

where a is the half width of the crack, $F(\xi)$ is the crack correction factor, $\Delta\sigma_d$ is the amplitude of the dynamic stress.

In states of low to medium stress, the Paris equation can simulate crack propagation well:

$$\frac{\mathrm{d}a}{\mathrm{d}N} = C(\Delta K)^m, \tag{2.20}$$

where N is the number of the vibration cycles, C and m are the material constants.

Under cyclic loading, the half width length of the crack after i cycles is as follows:

$$a_i = a_0 + \sum_{j=1}^{i}\Delta a_j, \tag{2.21}$$

where a_0 is the initial half width of the crack.

When estimating vibration fatigue life of thin plate structures with cracks, three failure criteria are used: frequency, half width, and strength (Ostiguy & Evan-Iwanowski, 1982; Shih & Wu, 2002):

1) when the first natural frequency of a cracked thin plate decreases by 5 %, the plate fails,
2) when the relative half width of the crack reaches 5 %, fatigue failure occurs in the plate,
3) when the stress intensity factor reaches material fracture toughness, fatigue failure occurs in the plate.

3. Numerical simulation analysis

The numerical simulation analysis is applied to verify the correctness and feasibility of the theoretical method proposed in this paper. The geometric model and mesh model of the plate

with a transverse crack are established by ANSYS. The crack is simulated by the discontinuity of meshes, and the crack will be always in an open state. In order to objectively describe breathing behaviour of the alternating open-closed crack in a vibration environment, the contact elements are established on both surfaces of the crack. The presence of contact elements prevents the intersection of the crack grids when crack surfaces come into contact, which effectively simulates breathing behaviour of the crack alternating open-closed.

The cracked plate is simply supported on all edges, and the dimensional drawing and finite element model are as shown in Figs. 2 and 3. Geometric sizes of the cracked plate are as follows: $l_1 = 1\,\mathrm{m}$, $l_2 = 0.5\,\mathrm{m}$, $h = 0.01\,\mathrm{m}$, $a_0 = 0.01\,\mathrm{m}$, $\rho = 2770\,\mathrm{kg/m^3}$, Young's modulus (20°) is $E_{20\,^\circ\mathrm{C}} = 69\,\mathrm{GPa}$. Young's modulus at different temperatures can be obtained:

$$E_T = \alpha E_{20\,^\circ\mathrm{C}}, \tag{3.1}$$

where α is a scale factor, $\alpha = -17.2\times10^{-12}T^4 + 11.8\times10^{-9}T^3 - 34.5\times10^{-7}T^2 + 15.9\times10^{-5}T + 1$.

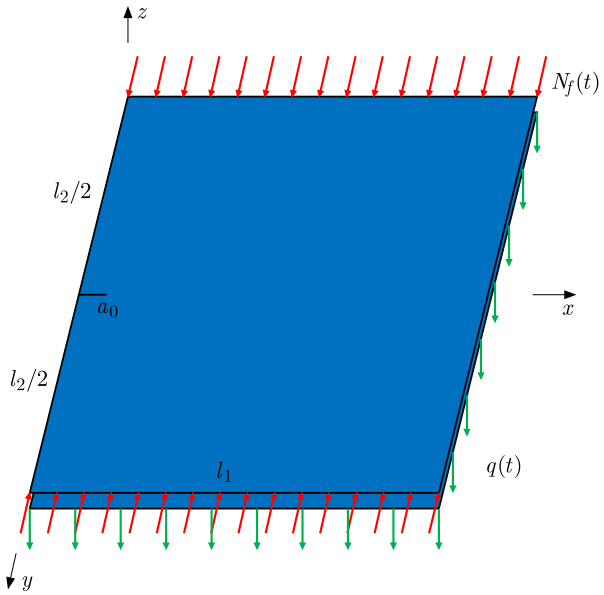

Fig. 2. Geometric dimensions of cracked plate .

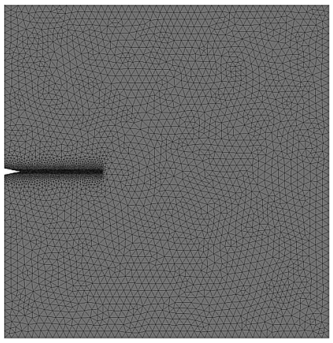

Fig. 3. Finite element model of cracked plate.

4. Results and discussion

4.1. Validation

Assuming that the cracked plate is actuated by two period excitations, one excitation is the in-plane force $N_f(t) = N_0 + N_t \cos\omega_1 t$, and the other is a uniformly distributed load $q(t) = q_t \cos\omega_2 t$ in the z-direction. The natural frequency of the first mode lateral vibration (Ostiguy & Evan-Iwanowski, 1982) is as follows:

$$\omega_L = \omega_T \left(1 - \frac{N_0}{N_{cr}}\right)^{1/2}, \tag{4.1}$$

where ω_T is the natural frequency of the plate, $N_{cr} = \frac{\pi^2 D}{l_1^2(2l_2/l_1 + l_1/2l_2)^2}$ is the static critical load.

The dimensionless natural frequencies can be derived as follows:

$$\Omega = \omega_L a^2 \sqrt{\rho h / D}, \tag{4.2}$$

where ω_L is the linear natural frequency of the cracked plate.

As shown in Table 1, for the non-destructive plate, the maximum error of the first order natural frequencies is less than 0.51 %, compared with the results in (Ostiguy & Evan-Iwanowski, 1982), and the first natural frequency error obtained by the numerical simulation method is lower. Therefore, for modal analysis of the plate, the theoretical method proposed in this paper has really high computational accuracy.

Table 1. Dimensionless natural frequencies of the plate without cracks.

Aspect ratios	a/l_1	N_0/N_{cr}	Ostiguy and Evan-Iwanowski (1982)	Theoretical	Numerical	Error rate [%]
$l_1/l_2 = 1$	0	0.2	17.66	17.572	17.60	0.49
		0.4	15.29	15.218	15.24	0.47
		0.6	12.48	12.425	12.45	0.44
$l_1/l_2 = 2$	0	0.2	44.14	43.914	43.97	0.51
		0.4	38.22	38.031	38.12	0.49
		0.6	31.21	31.052	31.15	0.51

As shown in Table 2, for the plate with different depth of cracks, the maximum error of the first order natural frequencies is less than 1.88 %, compared with the results in (Shih & Wu, 2002), and the first natural frequency error obtained by the numerical simulation method is lower. Therefore, for modal analysis of the cracked plate, the theoretical method proposed in this paper has sufficiently high computational accuracy.

Table 2. Dimensionless natural frequencies of the cracked plate.

Aspect ratios	a/l_1	N_0/N_{cr}	Shih and Wu (2002)	Theoretical	Numerical	Error rate [%]
$l_1/l_2 = 1$	0.01	0.2	17.62	17.579	17.59	0.23
		0.4	15.15	15.223	15.21	0.48
		0.6	12.20	12.430	12.30	1.88
$l_1/l_2 = 2$	0.01	0.2	44.25	43.959	44.12	0.66
		0.4	38.13	38.070	38.82	0.16
		0.6	30.95	31.084	31.02	0.43

4.2. Temperature field

Let us assume that the cracked plate is actuated by the temperature field, and the temperatures are as follows: $-20°$, $20°$, $50°$, $100°$. First order natural frequencies and dimensionless natural frequencies obtained by the theoretical method proposed in this paper are as shown in Table 3.

As shown in Table 3, the influence of the temperature field on the first order natural frequencies and dimensionless natural frequencies is significant and cannot be ignored. The natural frequency of the plate varies considerably when the temperature is within the two ranges $[-20°, 20°]$ and $[50°, 100°]$. Under the same temperature field, as the in-plane load ratio increases, the first order natural frequency of the cracked plate gradually decreases.

Table 3. Dimensionless natural frequencies of the cracked plate at different temperatures.

Aspect ratios	a/l_1	Temperature [°C]	ω_T [rad/s]	N_0/N_{cr}	$\Omega = \omega_L a^2\sqrt{\rho h/D}$
$l_1/l_2 = 1$	0.05	−20	300.0158	0.2	17.8085
				0.4	15.4226
				0.6	12.5925
		20	297.1507	0.2	17.5974
				0.4	15.2398
				0.6	12.4432
		50	297.2512	0.2	17.5972
				0.4	15.2396
				0.6	12.4431
		100	296.2710	0.2	17.6205
				0.4	15.2598
				0.6	12.4596

4.3. Dynamic response analysis

Let us assume that the cracked plate is under a uniformly distributed load $q(t) = q_t \cos\omega_2 t$, where $q_t = 0.8\,\mathrm{kN/m^2}$, and excitation frequencies are $\omega_{-20\,^\circ\mathrm{C}} = 300.0158\,\mathrm{rad/s}$, $\omega_{20\,^\circ\mathrm{C}} = 297.1507\,\mathrm{rad/s}$, $\omega_{50\,^\circ\mathrm{C}} = 297.2512\,\mathrm{rad/s}$, $\omega_{100\,^\circ\mathrm{C}} = 296.2710\,\mathrm{rad/s}$. When the temperature field is −20°, 20°, 50°, 100°, the vibration responses of the cracked plate are shown in Fig. 4 to Fig. 6.

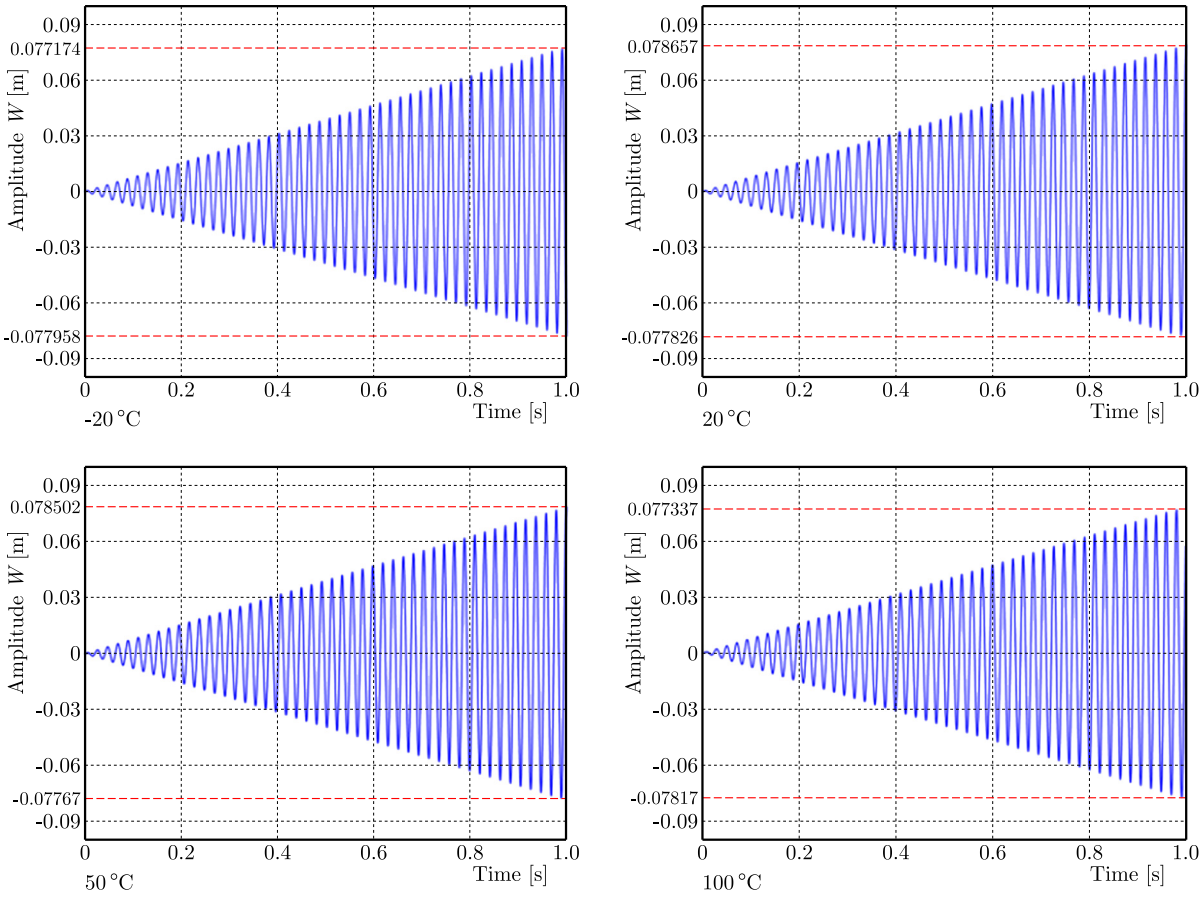

Fig. 4. Vibration response of the cracked plate when $\omega_2 = 300\,\mathrm{rad/s}$, $297\,\mathrm{rad/s}$, $297\,\mathrm{rad/s}$, $296\,\mathrm{rad/s}$.

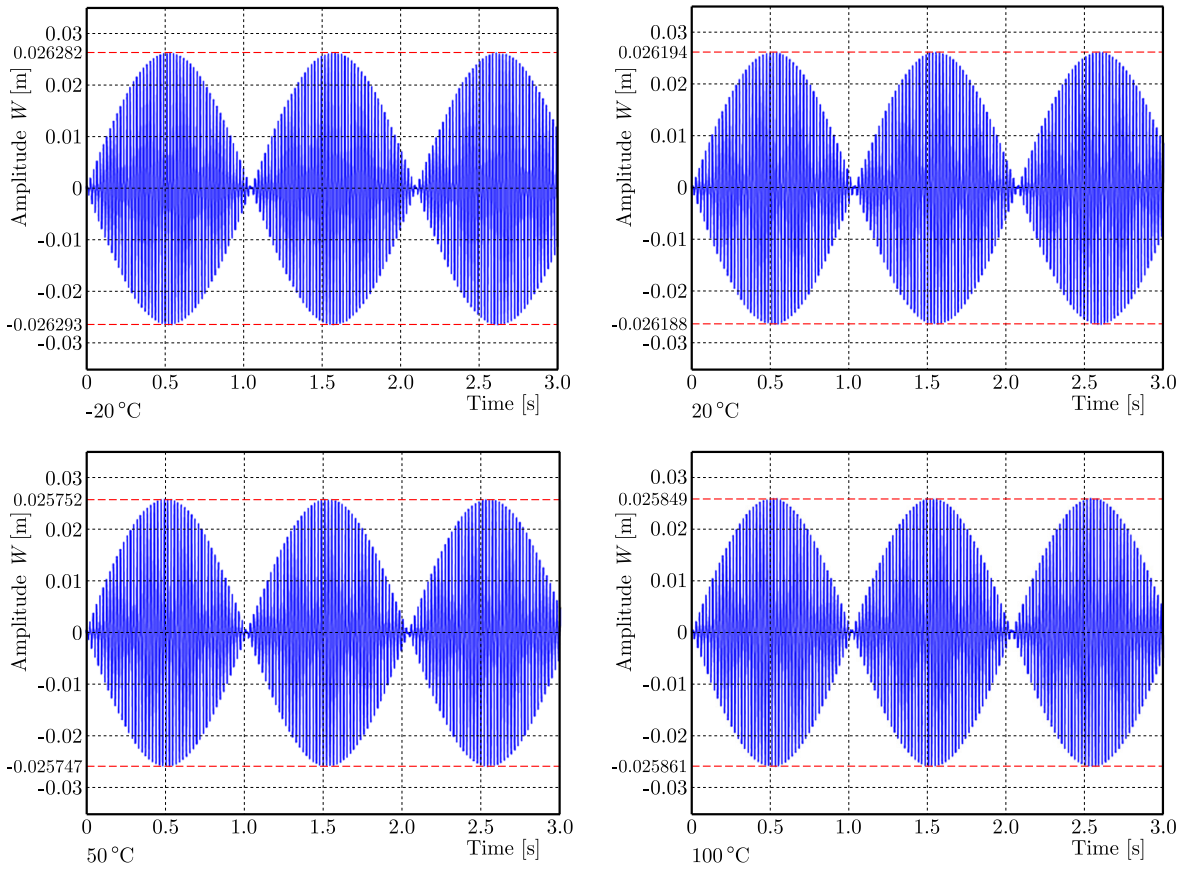

Fig. 5. Vibration response of the cracked plate when ω_2 is 0.98 times the natural frequency.

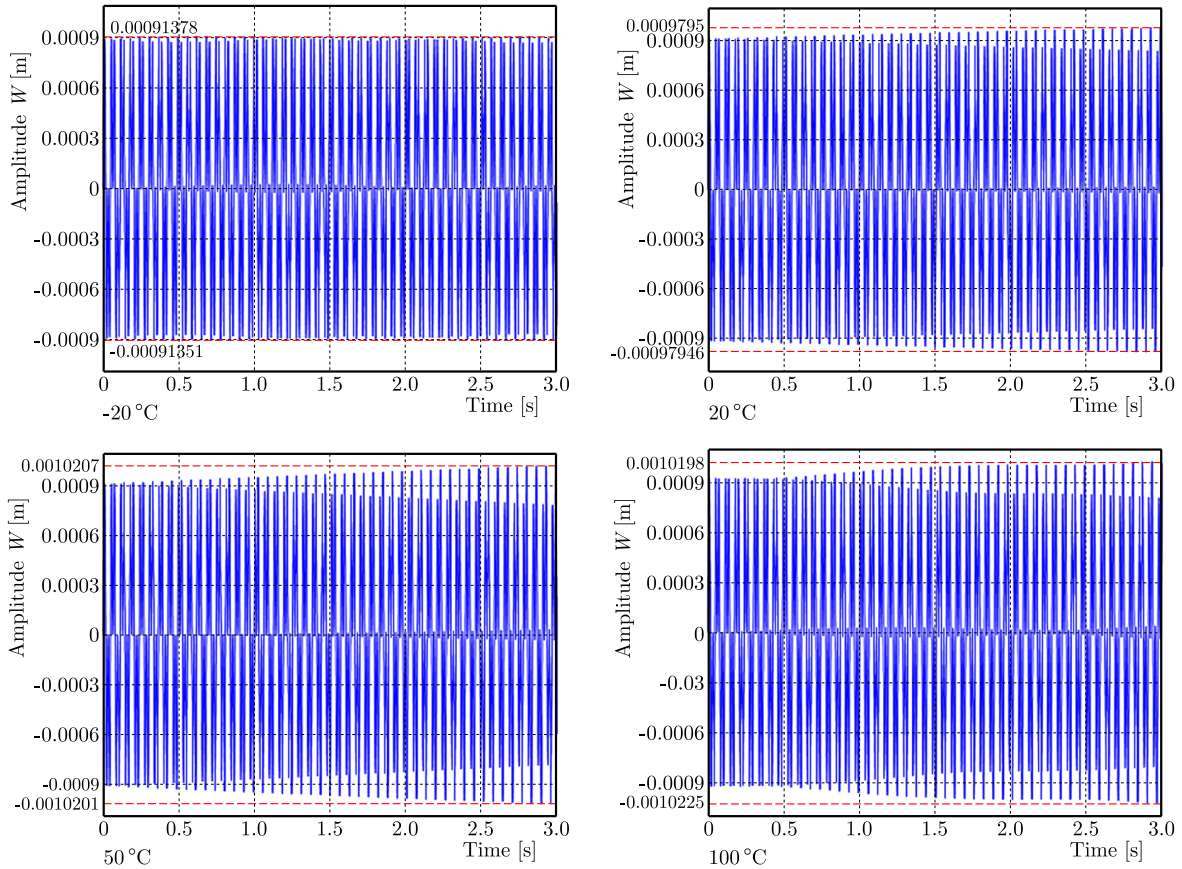

Fig. 6. Vibration response of the cracked plate when ω_2 is 1/3 times the resonant frequency.

As shown in Fig. 4 to Fig. 6, the influence of the external excitation frequency and temperature field on the vibration response of the cracked plate is significant. In Fig. 4, external excitation frequencies ω_2 are replaced by first order natural frequencies 300 rad/s, 297 rad/s, 297 rad/s, 296 rad/s, and the cracked plate will experience resonance phenomena, which causes the vibration amplitude to increase exponentially. In Fig. 5, the external excitation frequency ω_2 is 0.98 times the first order natural frequency, and the vibration response of the cracked plate exhibits a beat phenomenon. As the temperature increases, the beat period gradually shortens. In Fig. 6, the external excitation frequency ω_2 is 1/3 of the first order natural frequency, and the vibration response of the cracked plate exhibits a general response phenomenon.

4.4. Fatigue life analysis

Let us assume that the cracks' initial half widths are 0.03 m, 0.05 m, and 0.07 m, and temperature fields are $-20°$, $20°$, $50°$, $100°$. The external excitation is $q(t) = q_t \cos \omega_2 t$, and $q_t = 10\,\mathrm{N/m^2}$. The material constants are as follows: $C = 1.17 \times 10^{-12}$, $m = 3.447$ (Shih & Wu, 2002). Vibration fatigue life curves of the cracked plate derived by the theoretical method proposed are shown in Fig. 7. The crack propagation process of the plate obtained by the numerical method is shown in Fig. 8, and fatigue life comparison obtained by theoretical and numerical methods is shown in Table 4.

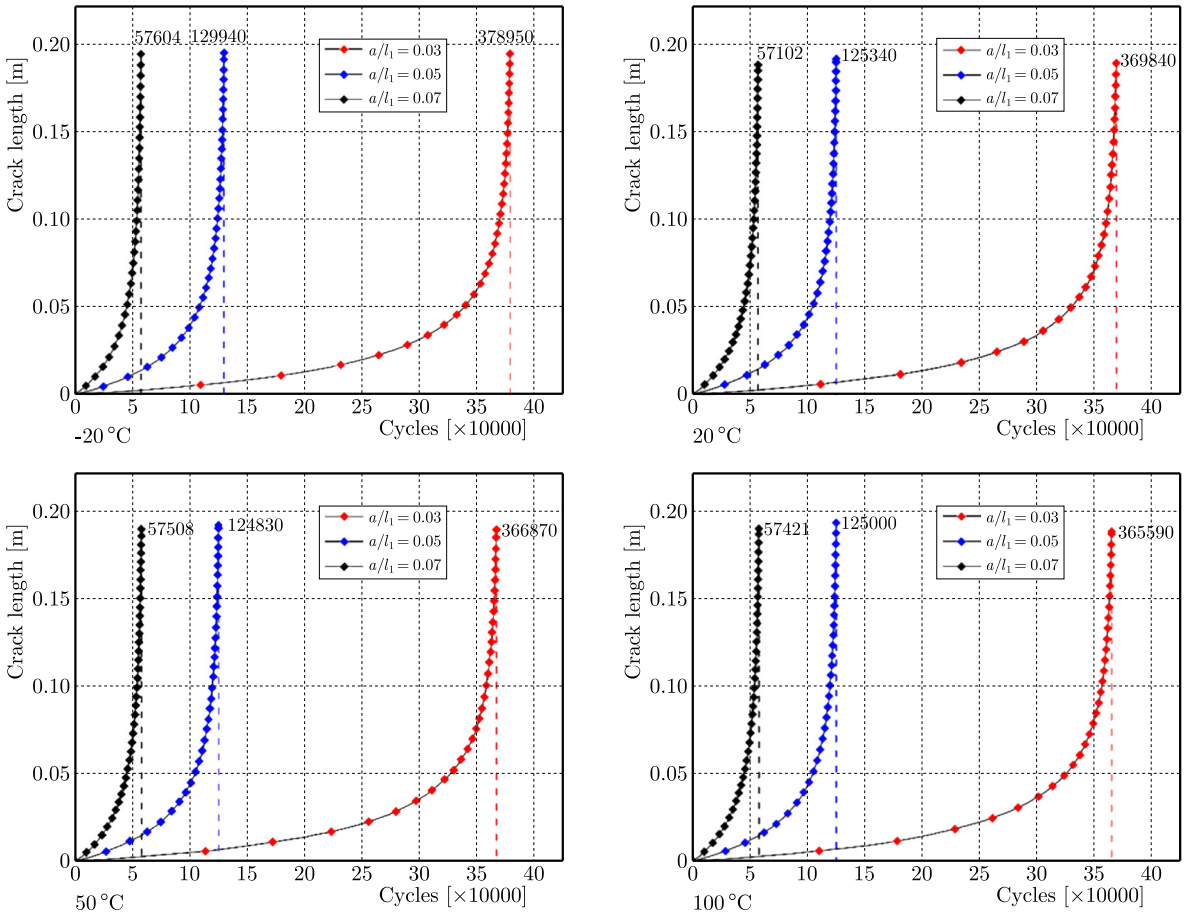

Fig. 7. Fatigue crack growth diagram of a cracked plate with different initial crack length.

As shown in Figs. 7 and 8, the temperature field has a certain influence on the vibration fatigue life of the cracked plate, but the initial mid width of the crack has a significant impact. As the initial half width of the crack increases, the vibration fatigue life rapidly decreases.

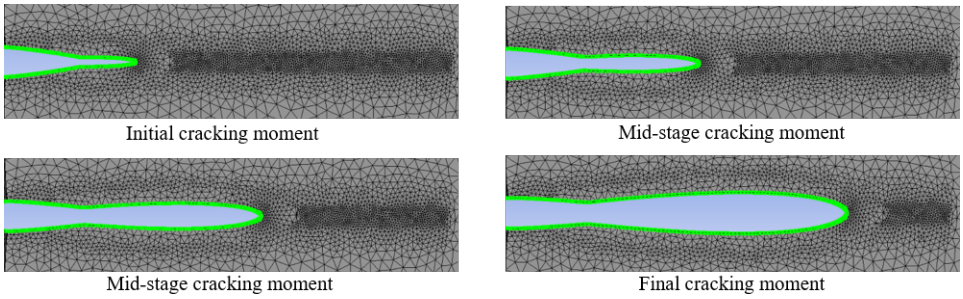

Fig. 8. Cracking process of the fatigue crack.

Table 4. Number of load cycles with a crack length of 0.2 m (×10 000).

a/l_1	−20°		20°		50°		100°		Max error [%]
	Numerical	Theoret.	Numerical	Theoret.	Numerical	Theoret.	Numerical	Theoret.	
0.03	45.07	37.90	44.01	36.98	43.59	36.69	43.65	36.55	19.1
0.05	15.39	12.99	14.83	12.53	14.81	12.48	14.84	12.50	18.7
0.07	6.81	5.76	6.75	5.71	6.81	5.75	6.81	5.74	18.6

According to the data comparison in Table 4, there is a certain error between the fatigue life of the plate obtained by the theoretical method proposed and the numerical results, with the maximum error being 19.1 %. There are probably three reasons for the large error:

1) the crack theory model proposed in this paper differs from the numerical model, resulting in significant errors in the lifespan of thin plates,
2) the loose coupling analysis method assumes that the stress at the crack tip remains constant during each cycle, but in numerical analysis, the stress at the crack tip varies periodically, resulting in errors in the incremental expansion of the crack during each vibration cycle,
3) in numerical analysis, cracks exhibit alternating breathing behaviour of opening and closing, and meshes on both crack surfaces interfere, which affects the accuracy of fatigue life calculation.

5. Conclusions

In this paper, the loose coupling analysis method is proposed to conduct the vibration fatigue behaviour analysis of the cracked plate, and investigate the influence of the temperature field on the modal, dynamic response, and vibration fatigue life behaviour. The change in the temperature field alters the elastic modulus of the plate and causes additional temperature stress in the plate. Therefore, the influence of the temperature field on the vibration fatigue behaviour of thin plate structures cannot be ignored. Considering the interaction between thermal coupling and crack propagation, the loose coupling analysis method can effectively investigate the vibration fatigue behaviour of the cracked plate. The theoretical method proposed in this article provides a solution for the life estimation of thin plate structures in service, and also provides theoretical possibilities for the health monitoring of thin plate structures in service.

Acknowledgments

This work is supported by the Natural Key R&D Program of China (no. 2022YFC2806605) and the National Natural Science Foundation of China (no. 12402063).

References

1. Berger, H.M. (1955). A new approach to the analysis of large deflections of plates. *Journal of Applied Mechanics*, *22*(4), 465–472. https://doi.org/10.1115/1.4011138

2. Heo, J., Yang, Z., Xia, W., Oterkus, S., & Oterkus, E. (2020). Free vibration analysis of cracked plates using peridynamics. *Ships and Offshore Structures*, *15*(sup1), S220–S229. https://doi.org/10.1080/17445302.2020.1834266
3. Huang, T., Lu, H., McFarland, D.M., Li, W.L., Tan, C.A., Bergman, L.A., & Gong, J. (2018). Natural frequency veering and mode localization caused by straight through–cracks in rectangular plates with elastic boundary conditions. *Acta Mechanica*, *229*(10), 4017-4031. https://doi.org/10.1007/s00707-018-2195-2
4. Ilie, P., & Ince, A. (2022). Three-dimensional fatigue crack growth simulation and fatigue life assessment based on finite element analysis. *Fatigue & Fracture of Engineering Materials & Structures*, *45*(11), 3251–3266. https://doi.org/10.1111/ffe.13815
5. Israr, A. (2008). *Vibration analysis of cracked aluminium plates* (Publication No. glathesis:2008-261) [Doctoral dissertation, University of Glasgow]. Enlighten: Theses. https://theses.gla.ac.uk/261/
6. Jalili, S., & Daneshmehr, A.R. (2018). Statistical analysis of nonlinear response of rectangular cracked plate subjected to chaotic interrogation. *International Journal of Applied Mechanics*, *10*(03), Article 1850033. https://doi.org/10.1142/S1758825118500333
7. Jameel, A., & Harmain, G.A. (2019). Fatigue crack growth analysis of cracked specimens by the coupled finite element-element free Galerkin method. *Mechanics of Advanced Materials and Structures*, *26*(16), 1343–1356. https://doi.org/10.1080/15376494.2018.1432800
8. Moradi, S., Makvandi, H., Poorveis, D., & Shirazi, K.H. (2019). Free vibration analysis of cracked postbuckled plate. *Applied Mathematical Modelling*, *66*, 611–627. https://doi.org/10.1016/j.apm.2018.10.004
9. Motaharifar, F., Ghassabi, M., & Talebitooti, R. (2021). A variational iteration method (VIM) for nonlinear dynamic response of a cracked plate interacting with a fluid media. *Engineering with Computers*, *37*(4), 3299–3318. https://doi.org/10.1007/s00366-020-00998-w
10. Ostiguy, G.L., & Evan-Iwanowski, R.M. (1982). Influence of the aspect ratio on the dynamic stability and nonlinear response of rectangular plates. *Journal of Mechanical Design*, *104*(2), 417–425. https://doi.org/10.1115/1.3256362
11. Rice, J.R., & Levy, N. (1972). The part-through surface crack in an elastic plate. *Journal of Applied Mechanics*, *39*(1), 185–194. https://doi.org/10.1115/1.3422609
12. Shih, Y.-S., & Wu, G.-Y. (2002). Effect of vibration on fatigue crack growth of an edge crack for a rectangular plate. *International Journal of Fatigue*, *24*(5), 557–566. https://doi.org/10.1016/S0142-1123(01)00110-4
13. Song, Y., Xue, K., & Li, Q. (2022). A solution method for free vibration of intact and cracked polygonal thin plates using the Ritz method and Jacobi polynomials. *Journal of Sound and Vibration*, *519*, Article 116578. https://doi.org/10.1016/j.jsv.2021.116578
14. Tazoe, K., Tanaka, H., Oka, M., & Yagawa, G. (2020). Analyses of fatigue crack propagation with smoothed particle hydrodynamics method. *Engineering Fracture Mechanics*, *228*, Article 106819. https://doi.org/10.1016/j.engfracmech.2019.106819
15. Useche, J. (2020). Fracture dynamic analysis of cracked Reissner plates using the boundary element method. *International Journal of Solids and Structures*, *191–192*, 315–332. https://doi.org/10.1016/j.ijsolstr.2020.01.017
16. Xue, J., & Wang, Y. (2019). Free vibration analysis of a flat stiffened plate with side crack through the Ritz method. *Archive of Applied Mechanics*, *89*(10), 2089–2102. https://doi.org/10.1007/s00419-019-01565-6
17. Xue, J., Wang, Y., & Chen, L. (2020). Nonlinear vibration of cracked rectangular Mindlin plate with in-plane preload. *Journal of Sound and Vibration*, *481*, Article 115437. https://doi.org/10.1016/j.jsv.2020.115437
18. Yadzhak, N., Andreykiv, O., & Lapusta, Y. (2022). Modelling small fatigue crack propagation under mixed mode II+III loading. *Procedia Structural Integrity*, *36*, 401–407. https://doi.org/10.1016/j.prostr.2022.01.052

Manuscript received June 20, 2025; accepted for publication November 3, 2025; published online February 10, 2026.